

Platinic metal porphyrins and hybrid nanomaterials embedding them as catalysts in chemical transformations

Anca Lascu*

*Institute of Chemistry "Coriolan Dragulescu" of Romanian Academy, M. Viteazul Ave, No. 24,
300223-Timisoara, Romania*

Email: ancalascu@yahoo.com, alascu@acad-icht.tm.edu.ro

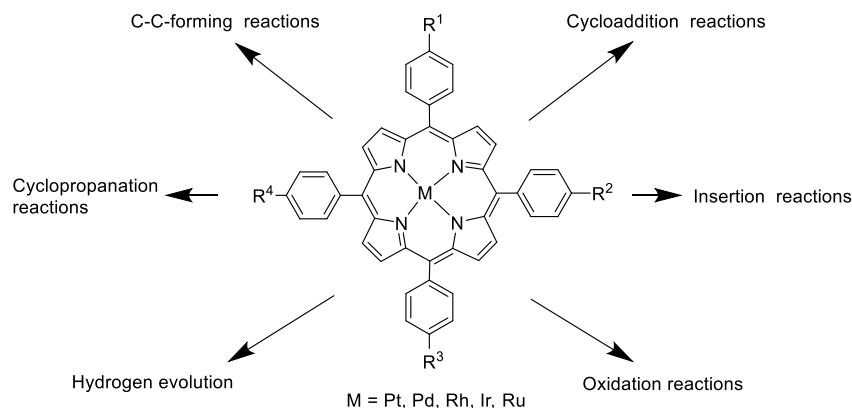
Received 08-05-2020

Accepted 09-15-2020

Published on line 10-02-2020

Abstract

The flat geometry of the porphyrin macrocycle and its extended conjugation allows for fine tuning the donating ability of the pyrrole rings via peripheral substituents. Platinic metal complexes with such ligands are thus ideally suited for redox reactions, as well as conventional organic transformations forming C-C bonds. Immobilization of such catalysts on crosslinked organic polymers yields active hybrid nanomaterials which retain significant catalytic activity and may be easily separated from the reaction mixture. Recent applications of both soluble and solid-supported catalysts in this class will be reviewed in this article.



Keywords: Platinic metal porphyrins, hybrid nanomaterials, catalysis, organic transformations

Table of Contents

1. Introduction
 2. Pd-porphyrins and their Hybrid Nanomaterials Catalysing Organic Reactions
 - 2.1 C-C forming reactions
 - 2.2 Borylation reactions
 - 2.3 Cycloaddition reactions
 - 2.4 Oxidation reactions
 3. Hybrid Nanomaterials Containing Rh-, Ru- and Ir-porphyrins as Catalysts in Organic Reactions
 - 3.1 CO₂ reduction
 - 3.2 Cyclopropanation reactions
 - 3.3 Hydroxylation of hydrocarbons
 - 3.4 Amination reactions
 - 3.5 Insertion reactions
 - 3.6 Oxidation reactions
 4. Hydrogen Evolution and Water Oxidation Catalysed by Pt- and Pd-porphyrin Hybrids
 5. Conclusions
 6. Acknowledgements
- References

1. Introduction

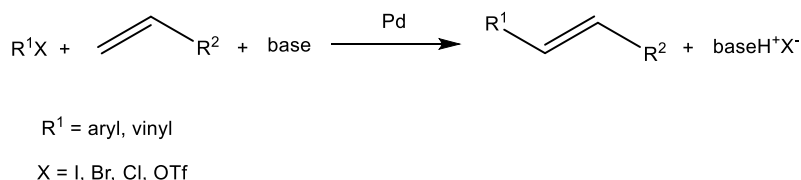
Improving the yield of a chemical reaction and reducing the costs by creating milder and more ecological conditions is an ongoing target of researchers all over the world. The main characteristics of a good catalyst are: high activity and selectivity, mechanical and thermal stability, easy separation and recovery, reusability. In the case of the reactions creating new C-C bonds, most catalysts rely on platinic metals, such as: platinum, palladium, rhodium, iridium and ruthenium. The extended aromatic π -conjugated macrocycles of porphyrins, their capacity for chemical functionalization by peripheral substitution as well as their capacity to accept metal ions in the centre of the molecule, their thermal stability make them excellent candidates to be tested as catalysts in various organic reactions. The porphyrin molecule can be designed such as to accommodate the active metal ion in the most favourable fashion, so that the access of the reacting molecules to the active site of the catalyst is not hindered, and the activity of the metal can also be enhanced by the surrounding substituents.

Platinum is a Group VIII transition metal; the properties of this metal are similar to Pd, even though Pt is larger in size due to its complete 4f orbital. The position of divalent platinum and palladium cations in the porphyrin molecule varies from within the porphyrin plane to above the plane, and also at the periphery of the macrocycle. The typical geometry of these metalloporphyrins is square planar.¹ Ruthenium and Rhodium are transition elements with incomplete 4d shell, their position in the porphyrin centre favours the binding of axial ligands, thus creating ideal catalytic sites. This review presents some important reactions that are catalyzed by platinic metal porphyrins and some of the best complexes that were used for this purpose.

2. Pd-porphyrins and their Hybrid Nanomaterials Catalysing Organic Reactions

2.1. C-C Forming reactions

Reductive Heck reaction between aryl halides and alkenes to form C(sp²)-C(sp²) bonds catalysed by palladium (Scheme 1) is highly enabling because it can forge alkyl-aryl linkages from widely available alkenes, rather than from the less accessible and/or more expensive alkyl halide or organometallic C(sp³) synthons that are needed in a classical aryl/alkyl cross-coupling. A general scheme for this C-C forming reaction:



Scheme 1. General Heck reaction.

As the reactivity of aryl halides decreases in the order: PhI > PhBr >> PhCl, the need to find more active catalysts for these type of aryl halides lead to the use of phosphine ligands and the increase in temperatures.

The quest for milder conditions and higher turnover numbers, better regioselectivity and efficiency favoured the abundance of palladium-based catalysts tested for this purpose. The optimum form in which palladium active sites are presented to the substrates varies largely in the attempt to prevent deactivation, and Pd(II)-porphyrins were recently tested as thermostable, air insensitive, phosphine-free, recyclable and efficient both homogeneous and heterogeneous catalysts.

The wide use of phosphine ligands for the catalysis of C-C coupling reactions stems partly from the electronic factors (in this case P vs N) and partly from the effect phosphine substituents have on the geometry and thus on the donating ability of the phosphorus centre. For instance, it is known that bulky alkyl ligands force a distortion of the typical tetrahedral geometry, changing the hybridization of the central donating atom and significantly increasing its s character. This alters redox potentials and transition state geometries also, markedly affecting the rates of oxidative addition and reductive elimination steps. Bidentate phosphine ligands can magnify these effects even further.

On the other hand, the relatively flat porphyrin ligands have a very limited degree of puckering around the donating environment. They are good ligands only for those atoms which can accommodate geometries such as square planar (sp²d hybridization, D_{4h} symmetry group, coordination number 4) or octahedral (sp³d², O_h symmetry group, coordination number 6). Open coordination sites and all of the factors mentioned previously are thus altered significantly. It is for this reason that the geometry of the porphyrin ligand, together with its electronic features stemming from the extensive conjugation altering the donating ability of the pyrrole rings, combine to make them more suitable as redox active ligands. This is reflected in HOMO and LUMO relative energies versus those of, for instance, phosphine ligands. Coupling this with extended π-conjugated systems suitable for light harvesting, or with bi-metal redox ligands of intermediate energies, allows for such reactions as water splitting which no conventional phosphine ligand could achieve.

Table 1. Catalysts used for the Heck coupling reaction

Catalyst	Conditions	%mol catalyst	Yields %	Reuse (runs)	Advantages /disadvantages	Ref.
Pd(II) tetra-(<i>N</i> -methyl-4-pyridinium)porphyrin iodide in <i>N</i> -butylpyridinium tetrafluoroborate ionic liquid	100 °C, 1 h	0.0025	100	7	-separation of the catalyst is difficult -the desired products are contaminated with heavy metals	2
Porphyrin 2A	DMF, K ₂ CO ₃ (2 mmol), 100 °C	0.05	TON over 1740	-	- high electron density at the Pd centre favours the coordination of the metal to aryl bromides	3
Porphyrin 2A locked in mesoporous SBA-15 silica	Et ₃ N; 140 °C, 4 h	0.1	100	9	- less effective for deactivated substrates	4
Porphyrin 2D grafted on graphene oxide activated by (3-chloropropyl)-trimethoxysilane	DMF, K ₂ CO ₃ (1.5 mmol), air atmosphere, 120 °C	10	Over 90	7	- it provides easy access to the catalytic sites and fast mass-transport of the reactants/products	7
Pd(II) tetra-(<i>N</i> -methyl-4-pyridinium)porphyrin iodide in Dowex 50WX8	DMF, K ₂ CO ₃ (2 mmol); 120 °C, 25 min	0.17 %mol Pd	90	5	-aryl halides with electron-withdrawing groups are more reactive	9
Pd(II) tetra-(<i>N</i> -methyl-4-pyridinium)porphyrin iodide in Amberlite IR-120	DMF, K ₂ CO ₃ (2 mmol); 120 °C, 38 min	0.34 %mol Pd	90	5	-Dowex 50 WX8 has a higher porosity	9
Porphyrin 2F immobilized on Amberlite IR-120	DMF, K ₂ CO ₃ (2 mmol), 120 °C, 21 min	0.83 mol% Pd	90	5	-the starting materials do not influence the reaction	10
Porphyrin 2F immobilized on Dowex 50 WX8	DMF, K ₂ CO ₃ (2 mmol), 120 °C, 16 min	0.75 mol% Pd	95	5	<i>trans</i> -products with 100% selectivity	10

For example, a catalytic system for the cross-coupling of aryl iodides and ethyl acrylate (Heck cross-coupling) was obtained by embedding palladium tetra-(*N*-methyl-4-pyridinium)- porphyrin iodide (Figure 1) in the ionic liquid *N*-butylpyridinium tetrafluoroborate, having similar pyridinium components.² (Table 1 entry 1)The homogeneous catalyst is recyclable but the separation of the expensive catalyst is difficult and the desired products are contaminated with heavy metals.

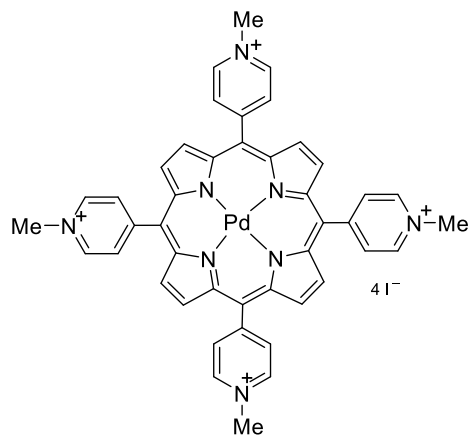


Figure 1. Pd(II) tetra-(*N*-methyl-4-pyridinium)porphyrin iodide.

The coupling between aryl bromides and alkyl acrylates with the obtaining of alkyl cinnamates (Mizoroki-Heck reaction) was attempted using a variety of palladium-porphyrins: Pd(II)-tetraphenylporphyrin, Pd(II)-tetra(*p*-cyanophenyl)porphyrin, Pd(II)-tetra(*p*-anisyl)porphyrin, Pd(II)-tetrasodium tetra(*p*-sulfonatophenyl)porphyrin (Figure 2A), Pd(II)-tetra(*p*-tolyl)porphyrin (Figure 2B), Pd(II)-tetra(*m*-hydroxyphenyl)porphyrin, and Pd(II)-tetra(*m*-carboxyphenyl)porphyrin (Figure 2G).³ (Table 1 entry 2) As model substrates the authors used 1-bromo-4-nitrobenzene and *tert*-butyl acetate. The results lead to the conclusion that a high electron density at the palladium centre favours the coordination of the metal to aryl bromides.

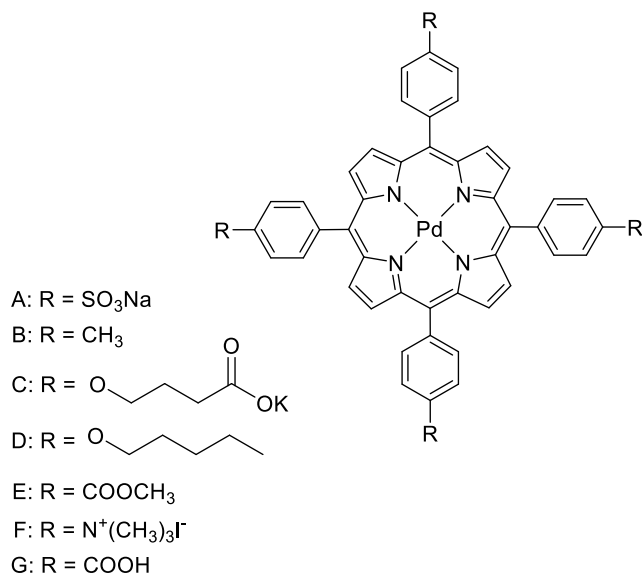


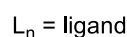
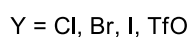
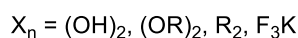
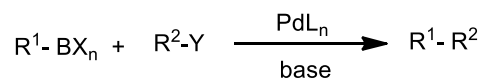
Figure 2. Pd(II)- A4-substituted porphyrins used as catalysts in organic reactions.

Another method to enhance the activity, stability and reusability of the Pd-porphyrin catalysts is their immobilization upon various thermo- and mechanically stable and porous supports, that enable the access of the reactant molecules to the active site of the Pd-catalyst itself.

A heterogeneous catalyst for the Heck reaction was obtained by functionalization of *N*-methylimidazole with Pd(II)-tetrasodium tetra(*p*-sulfonatophenyl)porphyrin (Figure 2A) (Table 1 entry 3) and its subsequent

locking into the channels of mesoporous SBA-15 silica material.⁴ The imidazolium cations act as linker between the silica material and the anionic porphyrin. The catalyst is efficient for the Heck reaction of aryl iodides/bromides and ethyl acrylate in absence of any organic ligand and organic solvent

Obtaining new C-C bonds for the synthesis of complex organic compounds can be performed by the cross-coupling reaction between organic boron compounds and organic halides, known as Suzuki–Miyaura coupling. This synthesis also requires palladium-based catalysts and a base for the activation of the boron compound and can be conducted under mild conditions.



Scheme 2. Suzuki–Miyaura coupling: general reaction.

The moisture insensitive, stable and nontoxic Pd(II)-tetra(*p*-tolyl)porphyrin (Figure 2B) (Table 1 entry 1) was able to catalyze the formation of new C-C bonds (Suzuki–Miyaura coupling reaction) in one pot.⁵ The best yield (93%) was obtained for the reaction between 4,4,5,5-tetramethyl-2-(4-nitrophenyl)-1,2,3-dioxaborolane and 4-bromoanisole obtaining pinacol arylboronates with high chemoselectivity. A large variety of substrates was tested and it was concluded that the catalyst presents a high tolerance for different functional groups of the substrate.

In an attempt to replace organic solvents for the Suzuki–Miyaura reaction with water, which enables the simple separation of the homogeneous catalyst, Skondra *et al.*⁶ obtained a water-soluble potassium carboxylate salt of a Pd(II)-porphyrin possessing butyrate antennae in the *para* position of the phenyl substituents of the porphyrin ring (Figure 2D) and used it as a pre-catalyst in cross-coupling reactions (Table 1 entry 2).

In order to obtain a heterogeneous catalyst with higher stability and easy recyclability, Bahrami *et al.*⁷ proceeded to the covalent grafting of Pd(II)-tetra-(*p*-hexyloxyphenyl)-porphyrin (Figure 2D) to the surface of graphene oxide activated by (3-chloropropyl)trimethoxysilane (Table 1 entry 3). This layered material was fully characterized and used as catalyst for Suzuki-Miyaura and Mizoroki-Heck reactions. For the Mizoroki Heck reaction, the aryl halides containing electron-donating groups as well as electron-withdrawing groups could react with styrene in yields of over 90%. The two-dimensional layered structure of the nanomaterial used as catalyst is responsible for its high activity because it provides easy access to the catalytic sites and fast mass-transport of the reactants/products.

The carbon–carbon coupling reaction using aryl halides and phenylboronic acid (Suzuki reaction) can be efficiently catalyzed by *meso*-tetra-[*p*-(methoxycarbonyl)phenyl]porphyrinato-palladium(II) (Figure 2E) supported on graphene oxide nanosheets.⁸ The palladium porphyrin was immobilized on the surface of the graphene by covalent bonding (Table 1 entry 4) This novel catalyst was fully morphologically characterized. The biphenyl by-product is obtained in 1%. Water helps the process because it attacks the phenylboronic acid and facilitates the elimination of B(OH)₃. Some of the advantages of this catalyst are: high specific surface area, thermal and chemical stability, moderate reaction time, high yield, relatively low temperature and no leaching of the palladium.

Table 2. Catalysts used for the Suzuki–Miyaura coupling

Catalyst	Conditions	% mol catalyst	Yields %	Reuse (runs)	Advantages /disadvantages	Ref.
Porphyrin 2B	DMF, K ₂ CO ₃ (2 equiv), 3 h,	0.15	93	-	-nontoxic, moisture insensitive catalyst -reaction in one pot - products are easy to separate	5
Porphyrin 2D	Water, K ₂ CO ₃ (2.0 mmol), 100 °C	0.001		-	- replacing organic solvents with water -No recycling, loss of activity	6
Porphyrin 2D grafted on graphene oxide activated by (3-chloropropyl)-trimethoxysilane	EtOH/H ₂ O (2:1 v/v), K ₂ CO ₃ (1.5 mmol) 80 °C	0.1 mmol Pd	99	5	- sensitive to the reaction temperature	7
Porphyrin 2E on graphene nanosheets by covalent bonding	DMF/H ₂ O =2:1(v/v) K ₂ CO ₃ (1.5 mmol), 70 °C, 40 min	0.7 % mol Pd	Over 92%	7	- Water facilitates the elimination of B(OH) ₃ .	8
Pd(II) tetra-(<i>N</i> -methyl-4-pyridinium)porphyrin iodide in Dowex 50WX8	DMF/H ₂ O (2:1)v/v K ₂ CO ₃ (1.5 mmol) 95 °C-reflux, 7 min	0.13 mol% Pd	96	5	-stability to air and moisture	9
Pd(II) tetra-(<i>N</i> -methyl-4-pyridinium)porphyrin iodide in Amberlite IR-120	DMF/H ₂ O (2:1)v/v K ₂ CO ₃ (1.5 mmol) 110 °C, 17 min	0.27mol% Pd	97	5	- stability to air and moisture	9
Porphyrin 2F immobilized on Amberlite IR-120	DMF/H ₂ O (2:1v/v) K ₂ CO ₃ (1.5 mmol) 110 °C under air	0.59 mol% Pd	97	5	- Amberlite is a cross-linked polymer with more restricted porosity	10
Porphyrin 2F immobilized on Dowex 50 WX8	DMF/H ₂ O (2:1v/v) K ₂ CO ₃ (1.5 mmol) 95 °C under air	0.43 mol% Pd	97	5	-high thermal stability	10

Embedding ionic palladium tetra-(*N*-methyl-4-pyridinium)porphyrin iodide (Figure 1) into Dowex 50WX8 and Amberlite IR-120 ion-exchange resins (Figure 3) via electrostatic interactions⁹ provided heterogeneous

catalysts for the reaction of aryl halides with styrene (Heck reaction) (Table 1 entry 5 and 6) and for the reaction of phenylboronic acid with aryl halides (Suzuki reaction) (Table 2 entry 5 and 6).

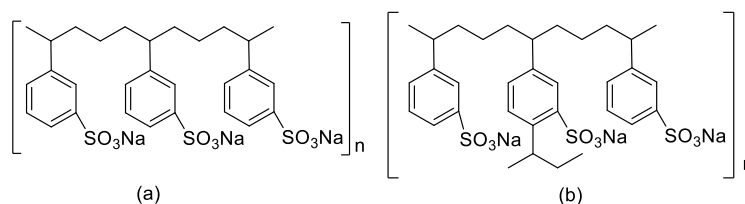


Figure 3. Structure of (a) Dowex 50WX8 and (b) Amberlite IR-120.

By supporting the porphyrin on the resins, the active sites of the catalyst are isolated and can improve their activity. The variety of aryl halides investigated, good to excellent yields, short reaction times and stability of these systems to air and moisture present advantages of these catalysts. The higher reactivity of the catalyst deposited on Dowex 50 WX8 can be attributed to its different structure and porosity as compared to Amberlite IR-120.

As other supports for the Heck cross-coupling reaction were tested, it was observed that aryl halides with electron-withdrawing groups are more reactive as compared to the aryl halides containing electro-donating substituents and that chloroarenes are less reactive than iodo- and bromo-arenes.

Another ionic Pd-metalloporphyrin, tetrakis(*N,N,N*-trimethyl-ammonium-phenylene)porphyrinato-Pd(II) iodide (Figure 2F), more substituted at the pyridinium nitrogen atom, was also immobilized on Amberlite IR-120 and Dowex 50 WX8 resins via electrostatic interactions by the same authors.¹⁰ The obtained catalysts were characterized by spectroscopic methods and it was confirmed that the immobilized Pd-porphyrin presents a high thermal stability.

For the Heck cross-coupling the optimum parameters are presented in (Table 1 entry 7 and 8).

The Suzuki–Miyaura cross-coupling of 4-iodoanisole with phenylboronic acid was also chosen as model coupling reaction (Table 2 entry 7 and 8). It can be observed that the amount of catalyst required for 96% yield is higher than in the case of using the Pd(II) tetra-(*N*-methyl-4-pyridinium)porphyrin iodide, proving the higher activity of the Dowex-supported catalyst, due to the fact that Amberlite is a cross-linked polymer with more restricted porosity. The investigations concerning different substituents on the aromatic rings of the starting materials showed that they do not influence the reaction.

The palladium-active site of the catalyst can also be present outside the porphyrin ring. For example, Osuka *et al.*¹¹ obtained porphyrin-based pincer complexes wherein the palladium is directly attached to a porphyrin carbon atom and to two phosphine donors (PCP-pincer) (Figure 4). The allylation of benzaldehyde with allyltin was chosen as model reaction to test the catalytic capacity of the pincer complex, because it proceeds with maintaining of the valence of the transition metal. The pincer containing M=Zn furnished a yield of 97% yield and when M=Ni the yield was 95%, using 1 mol% catalyst, 2 mol% AgPF₆, dimethylacetamide as solvent, 100 °C and 40 h. It can be observed that the amount of catalyst is large, the reaction time lengthy and the required temperature high.

More complex meso-tetra(SCS-pincer PdCl)-metalloporphyrin hybrids (Figure 5) were obtained by Klein Gebbink *et al.*¹² In this case the metal centre of the porphyrin was chosen from Mg, MnCl and Ni and the four peripheral metal ions are palladium. The four SCS-pincer ligand groups are substituted thiophenyl groups. The *tert*-butyl substituents have the purpose of increasing the solubility of the porphyrin. These complexes were used as precatalysts in the Heck reaction between iodobenzene and styrene in DMF at 119 °C with one equiv.

of iodobenzene, 1.5 equiv. of styrene, 1.5 equiv. of Et_3N , and 0.05 mol % of the respective pincer porphyrin. Among the investigated metalloporphyrins, the best-performing pincer hybrid coincides with the most electron-rich porphyrin ring, containing Mg, showing that the electron-donating properties of the porphyrin influences the catalytic properties of the peripheral Pd.

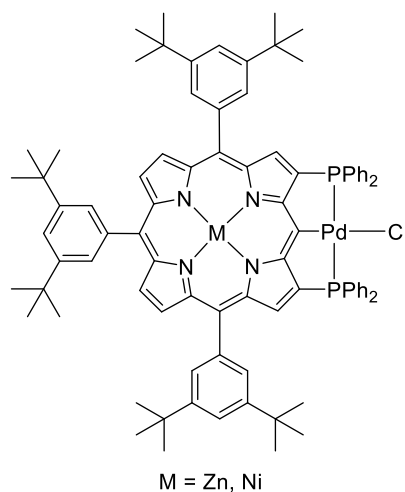


Figure 4. Porphyrin-based PCP pincer complex.

It can be concluded that Pd(II)-tetra-(*p*-hexyloxyphenyl)porphyrin possessing large substituents (Figure 2D), grafted to the surface of activated graphene oxide⁷ is an excellent choice of catalyst both for the Suzuki-Miyaura and for the Mizoroki Heck reactions, as it provides high yields (over 90%), uses small amounts of catalytic material, mild reaction conditions and good reusability of the heterogenous catalyst. Dowex-supported Pd(II)-porphyrins^{9,10} are also good catalysts for the C-C forming reactions, due to their high porosity and the better access of the reacting molecules to the active site of the catalyst.

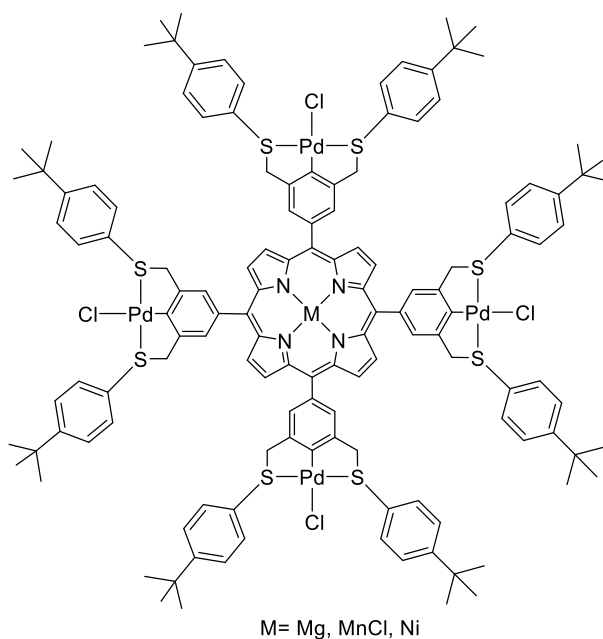
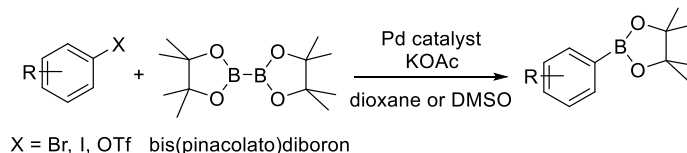


Figure 5. *meso*-Tetra(2,6-bis[(4-tert-butylphenylsulfido)methyl]-1-chloridopalladio(II)phenyl)-metalloporphyrin hybrid.

2.2. Borylation reactions

The Miyaura borylation reaction (Scheme 3) allows the obtaining of boronates. Arylboronate esters of diols or pinacol arylboronates are synthetic building blocks in organic chemistry because of their stability to air, moisture and temperature. They can be used as starting materials for the Suzuki coupling, without prior hydrolysis. The general reaction scheme for aryl halides is:



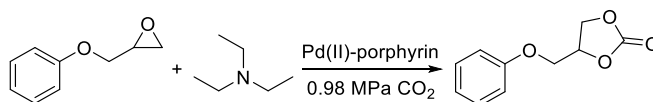
Scheme 3. General Miyaura borylation reaction.

As the palladium-based catalysts involve phosphine-based ligands, that are toxic, expensive and moisture and air sensitive, thus difficult to handle, other catalysts that can offer more stable nitrogen ligands are required.

Several Pd(II)-porphyrins were investigated by Rao *et al.*¹³ as promising catalyst for the Miyaura borylation: Pd(II)-tetra(*m*-hydroxyphenyl)porphyrin, Pd(II)-tetra(*m*-carboxyphenyl)porphyrin, Pd(II)-tetraphenylporphyrin, Pd(II)-tetrasodium-tetra(*p*-sulfonatophenyl)porphyrin, Pd(II)-tetra(*p*-cyanophenyl)porphyrin, Pd(II)-tetra(*p*-tolyl)porphyrin and Pd(II)-tetra(*p*-anisyl)-porphyrin. It was concluded that Pd(II)-tetra(*p*-tolyl)porphyrin (Figure 2B) was the compound that in 0.15 mol% gave highest yields when catalysing the reaction between 1-bromo-4-nitrobenzene and bis(pinacolato)diborane in the presence of potassium acetate to produce 4,4,5,5-tetramethyl-2-(4-nitrophenyl)-1,2,3-dioxaborolane in 92% yield, in 5 h in aerobic conditions. The compound Pd(II)-tetraphenylporphyrin shows no catalytic activity, and Pd(II)-tetra(*m*-carboxyphenyl) porphyrin furnishes low yields. The substrates containing electron-withdrawing groups can react better than the electron-rich ones. The authors also proposed a mechanism of action, implying a first step in which a Pd⁰ species is formed.

2.3. Cycloaddition reactions

A method to effect the fixation of carbon dioxide and to convert it into high-value products is the epoxide cycloaddition to CO₂, when cyclic carbonates, essential materials for the synthesis of polyurethanes, are obtained. Dela Cruz *et al.* considered the use of *N*-confused metalloporphyrins as catalysts for such reactions, on the basis that the peripheral nitrogen atom can be functionalized further and the internal carbon atom furnishes carbon-metal bonds.¹⁴ It was shown that 1,2-epoxy-3-phenoxypropane was converted into 4-(phenoxyethyl)-1,3-dioxolan-2-one in an 18-hour interval with a turnover number of 7000, at 120 °C, in an autoclave, in the presence of 0.015 mol% of a bifunctional Pd(II)-*N*-confused tetraphenylporphyrin (Figure 6) as catalyst, 6 mol% of triethylamine and CO₂ pressure of 0.98 MPa, in solvent-free conditions (scheme 4).



Scheme 4. Cycloaddition reaction.

It was suggested that the epoxide ring is activated both by the metal centre and the peripheral carboxylate group. Higher yields are obtained for epoxides that have electron-withdrawing substituents or substituents capable of van der Waals interactions with the peripheral functionality of the catalyst. Nevertheless, the authors attempted the introduction of a less expensive and more ecologically-benign metal in the core of the N-confused porphyrin ring, namely Ni, with the correction that 2,6-lutidine was introduced as the deprotonating base. Good yields (TON of up to 6500) were also obtained in this instance.

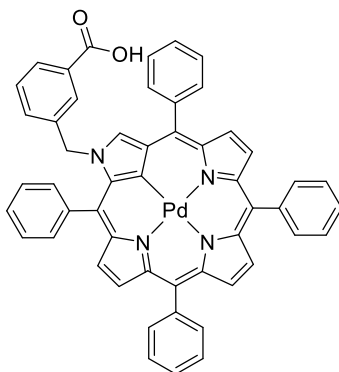
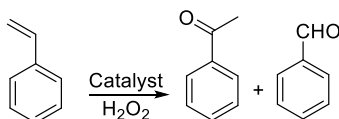


Figure 6. Pd(II)-N-confused tetraphenylporphyrin

2.4. Oxidation reactions

Another type of organic reaction that needs catalysts for control of the selectivity is oxidation. The selective oxidation of styrene to acetophenone and benzaldehyde (Scheme 5) was obtained for example using a metal-organic framework (MOF) that consists in Pd(II)-tetra(carboxyphenyl)porphyrin (Figure 2G) and cadmium(II) connecting nodes.¹⁵



Scheme 5. Oxidation of styrene.

Each Pd-porphyrin molecule acts as an octa-dentate ligand to coordinate eight Cd atoms of four neighbouring Cd chains into a three-dimensional structure. The oxidation reactions take place in acidic conditions, the nature and quantity of the acid determines the yield in acetophenone. The required temperature is 55 °C and the conversion is 100% after 12 h. The MOF offered high stability, easy separation and recyclability.

The photoinduced oxidative functionalization of tertiary amines and the photochemical oxidation of sulfides to sulfoxides were achieved using Pt(II)-tetra(pentafluorophenyl)porphyrin and Pd(II)-tetra(pentafluorophenyl)porphyrin (Figure 7) as efficient and robust catalysts.¹⁶ These compounds were chosen because of their strong absorption in the visible region, long-lived triplet excitation states and their stability to oxidative degradation. It was concluded that both perfluorinated metalloporphyrins are able to catalyse the light-induced aerobic oxidation of dibenzylamine to the corresponding imine in over 98% yield, within 2.5 h, despite the fact that the catalyst loading is very low (0.005 mol%). The irradiation took place with visible light wavelengths ($\lambda = 400$ nm) in aerobic conditions, in MeCN as solvent. The mechanism of the

oxidation was also proposed, as the photochemically generated singlet oxygen induces the oxidation of amine to iminium ion intermediate and this reacts with nucleophiles to give the corresponding products.

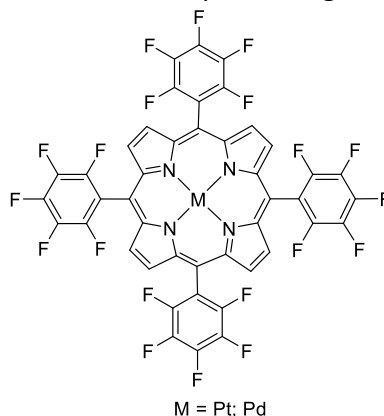


Figure 7. M(II)-tetra(pentafluorophenyl)porphyrin.

3. Hybrid Nanomaterials Containing Rh-, Ru- and Ir-porphyrins as Catalysts in Organic Reactions

An extensive review covering Rh-porphyrins was published in 2018, by Dong *et al.*¹⁷ The synthesis, properties, transformations and applications of various Rh-porphyrins were presented.

3.1. CO₂ reduction

More recent work regarding the use of hybrid nanomaterials containing Rh-porphyrins as catalysts in organic reactions was presented by Su *et al.*¹⁸ They obtained a metal-organic framework (MOF) by self-assembling Rh(III)-tetra(p-carboxyphenyl)porphyrin chloride (Figure 8) with ZrCl₄. This metal-organic framework contains single-sited unsaturated Rh-porphyrin units and was used as selective photocatalyst for CO₂ reduction to formate ion. The reduction of CO₂ was carried out using acetonitrile as reaction solvent and triethanolamine as sacrificial agent, under visible light irradiation ($\lambda \geq 400$ nm) in the absence of additional photosensitizer.

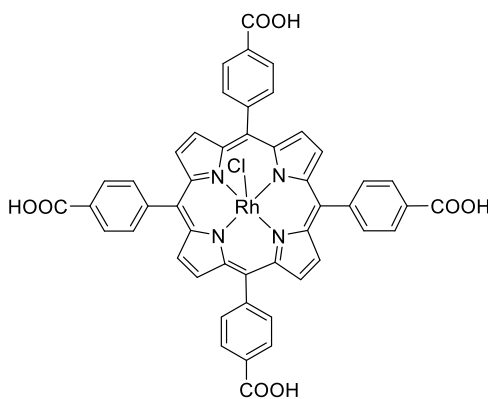


Figure 8. Rh(III)-tetra(p-carboxyphenyl)porphyrin chloride.

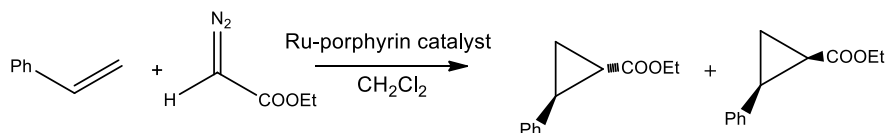
The amount of formate ion reached $6.1 \mu\text{mol}/\mu\text{mol}_{\text{cat}}$ in 18 h exposure to visible light irradiation and a turnover frequency of 0.34 h^{-1} , comparable to that of other MOF-based catalysts, MOF-253-Ru(CO)₂Cl₂.¹⁹ The selectivity of the reduction reaction resides in the fact that this Rh-porphyrin containing MOF has adequate adsorption capacity both for CO₂ and for CO, with strong bonds between CO and the Rh atoms and the CO₂[•] activated intermediate can combine easier with a hydrogen atom to form the formate ion. The robust and heterogeneous photocatalyst can be reused three times without loss of activity.

3.2. Cyclopropanation reactions

Obtaining the strained rings present in cyclopropanes requires highly reactive species, such as carbenes, ylids and carbanions on one of the reagents, both new bonds are being made to the same atom. Cyclopropanation of double bonds is usually catalysed by transition metals, especially Rh (II, III) compounds. The proven stability, recyclability along with the pocket-like environment around the catalytically active metalloporphyrin centre motivated Fischer *et al.*²⁰ to test Rh-porphyrin-containing metal-organic frameworks as heterogeneous catalysts for the cyclopropanation of olefins with ethyl diazoacetate. The metal-organic frameworks were obtained from saponified tetra(p-methoxycarbonylphenyl)porphyrinato-Rh(III) chloride and ZrCl₄ [PCN-224(Rh)] and from [tetra(p-carboxyphenyl)porphyrin-Rh(III) chloride (Figure 9) and ZrCl₄ [PCN-222(Rh)] respectively, by solvothermal synthesis in benzoic acid as modulator. The two MOF-s differ in pore geometry and topology and in the Rh–Rh distance, that for PCN-224(Rh) is 13.6 Å and for PCN-222(Rh) is 9.7 Å, but the Zr–Rh distances in both MOFs are identical. The authors optimized the conditions, using catalyst loadings of 0.0033 mmol (0.4 mol% Rh), excess olefin and a motorized pump for the introduction of ethyldiazoacetate in order to improve the yields. An extensive study regarding various olefin substrates and the catalyst-topology-dependent diastereoselectivity of the reactions is also presented.

Axial N-heterocyclic carbene (NHC) ligands on Ru-porphyrins are increasingly used in catalysis. Che *et al.* synthesized a series of ruthenium porphyrins having N-heterocyclic carbenes as axial ligands and tested them for a series of organic reactions such as: alkene cyclopropanation, carbene C-H, N-H, S-H, and O-H insertion, alkene aziridination, and nitrene C-H insertion.²¹ Owing to the strong donor strength of NHC ligands, these complexes show high catalytic activity towards alkene cyclopropanation, carbene C-H, N-H, S-H, and O-H insertion, alkene aziridination, and nitrene C-H insertion with turnover frequencies up to 1950 min^{-1} . The *trans* axial NHC ligand facilitates the decomposition of diazo compounds by stabilizing the metal–carbene reaction intermediate.

The catalytic cyclopropanation reaction (Scheme 6) of 1.6 mmol alkenes with 0.8 mmol ethyl diazoacetate, using 0.0004 mmol Ru(IV)-[tetra(4-fluorophenyl)porphyrin](1,3-dimethyl-2,3-dihydro-1H-benzimidazol-2-ylidene)₂ (Figure 15) as catalyst, in 1 mL CH₂Cl₂ proved to be the best reaction conditions, that led to yields higher than 78% after 20 minutes reaction time and a *trans/cis* ratio of 17/1 of the obtained products.



Scheme 6. General cyclopropanation of styrene

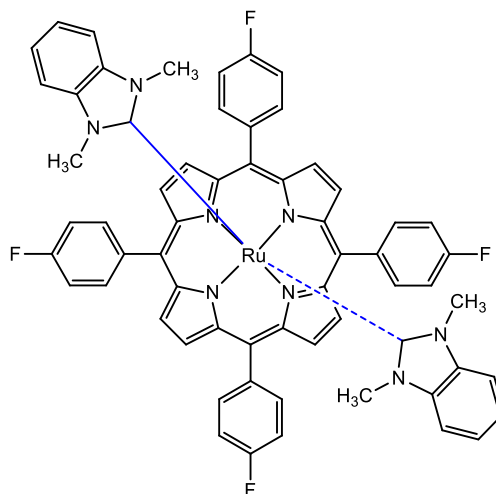


Figure 9. Ru(IV)-tetra(p-fluorophenyl)porphyrin(1,3-dimethyl-2,3-dihydro-1H-benzimidazol-2-ylidene)₂.

The reaction between styrene and ethyl diazoacetate in water to give cyclopropane esters was conducted with water soluble, optically active ruthenium porphyrins with yield 85%, high diastereoselectivity (*trans/cis*: 92/8) and good enantioselectivity for the *trans* isomer (83%).²² The porphyrin possesses as substituents C₂-symmetric groups which contain two norbornane groups fused to the central benzene ring - Halterman porphyrin. The sulfonated Halterman porphyrin (Figure 10) is water-soluble, optically active and can be reused as catalyst for four cycles.

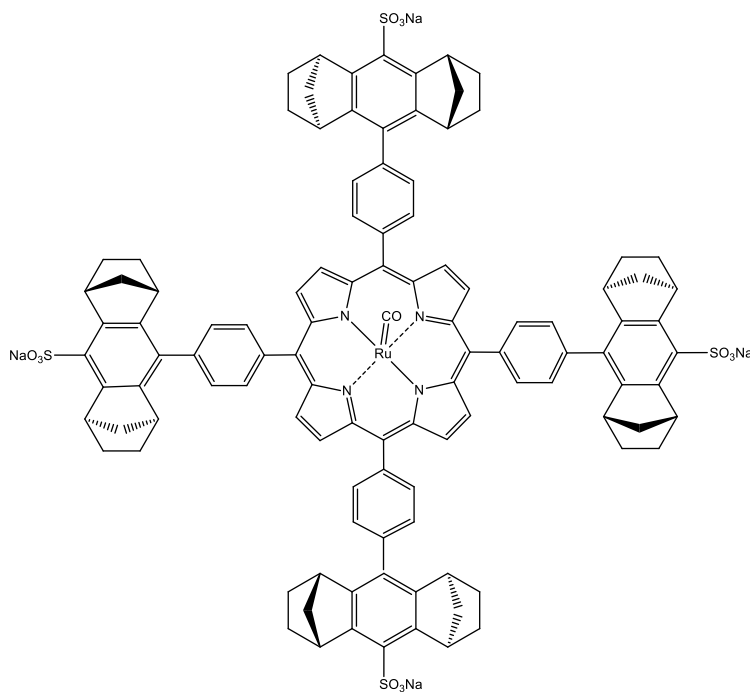


Figure 10. Sulfonated Halterman porphyrin.

The ruthenium complexes of phthalocyanine macrocycles have robust chemical properties and are therefore good candidates as catalytic systems for cyclopropanation of styrenes and in the carbene insertion to N-H bond of anilines using ethyl diazoacetate (EDA) as a carbene donor. Sorokin *et al.*²³ obtained Ru(III)- and Ru(IV)-octa-*n*-butoxyphthalocyanine complexes from Ru₃(CO)₁₂ and the corresponding octa-*n*-butyloxy-

phthalocyanine under reflux in *o*-dichlorobenzene. The obtained products included a monomeric Ru(III) complex having a CO molecule axially coordinated and a dimeric phthalocyaninato-Ru(IV) complex with μ -carbido bridge having a sandwich-like structure (Figure 11). This μ -carbido diruthenium complex was used as catalyst for the cyclopropanation of olefins by EDA and yields of 100% were obtained for substrates like *p*-methoxystyrene and 1,1-diphenylethene in toluene under argon, at 90 °C, in 6 hours. The reaction of *N*-H insertion of EDA to amines catalysed by μ -carbido diruthenium complex yielded 100% product when starting from aniline, *p*-methylaniline and *p*-chloroaniline in toluene at 90 °C.

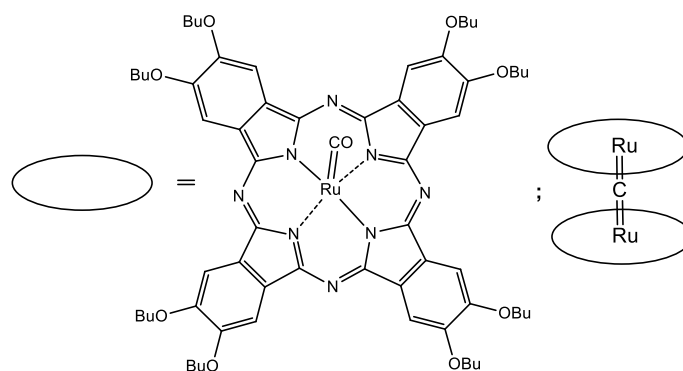


Figure 11. Monomeric octabutoxyphthalocyaninoruthenium(II) carbonyl complex and dimeric μ -carbido bis[octabutoxyphthalocyaninoruthenium(IV)] complex.

Metalloporphyrin complexes with 2-adamantylidene axial ligands (Figure 12) display thermal and chemical stability due to the synergistic effect of the metal-carbene bond.²⁴ This type of compounds can act as catalysts for intermolecular diarylcarbene transfer reactions including cyclopropanation and X-H (X = S, N, O, C) insertion reactions. The best yields are provided by the compounds containing Fe as central metal ion, but the Ru-containing compound reached 92% yield in catalysing carbene transfer reactions, under mild conditions: dichloromethane, 40 °C and 12 hours.

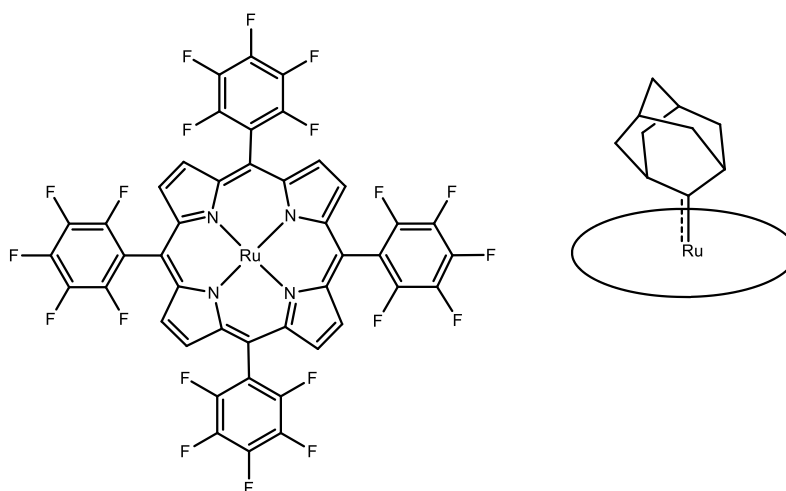


Figure 12. Ru(IV)-tetra(pentafluorophenyl)porphyrin having a 2-adamantylidene axial ligand.

An extensive review concerning the synthesis, structure, reactivity and catalytic activity of carbene Ru/Os porphyrins was presented by Che and Huang.²⁵ The porphyrin ligands are *meso*-tetraarylporphyrinato

dianions. The structures of the Ru and Os porphyrin carbene complexes were characterized by X-ray diffraction and mass spectrometry. It was concluded that they are active intermediates toward catalytic cyclopropanation of alkenes or stoichiometric saturated C/H insertion of unfunctionalized alkenes and the first examples of metalloporphyrin carbene complexes that bear monosubstituted carbene groups CHR, or contain multiple carbene ligands at the axial sites.

3.3. Hydroxylation of hydrocarbons

An extensive study regarding the hydroxylation of hydrocarbons with 2,6-dichloropyridine *N*-oxide as oxidant was performed by using ruthenium complexes of tetra(pentafluorophenyl)porphyrin (Figure 13) as catalysts.²⁶ High turnover numbers were reported, up to 14800 in the case of adamantane as substrate. The authors used mild reaction conditions (CH₂Cl₂ solvent, highest temperature 65 °C) and small quantities of catalyst (1 × 10⁻⁸ M) for the reaction. The proposed mechanism of reaction implies a fast cycle involving metastable Ru(III) and oxoRu(V) intermediates and a slow oxidation cycle, mediated by oxoRu(IV) and trans-dioxoRu(VI) porphyrin complexes.

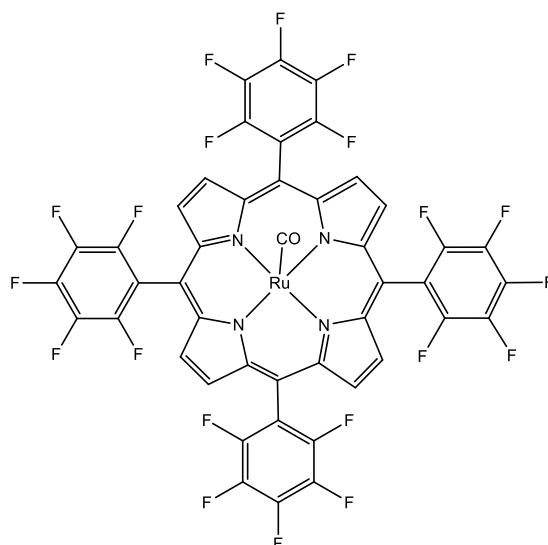


Figure 13. Ruthenium (II)-tetra(pentafluorophenyl)porphyrin carbonyl.

3.4. Amination reactions

The direct transfer of a nitrene moiety to hydrocarbons, amination reaction, can be catalysed by metalloporphyrin complexes, that leads to chemo-, stereo-, and even enantioselectivity using any nitrene source. An extensive perspective on the subject was presented by Gallo *et al.*²⁷

Nitrene transfer reactions (amination reactions) with the formation of aza-derivatives were catalysed by sandwich-type ruthenium(IV) μ -oxo porphyrin complexes (Figure 14).²⁸ The yields exceed 44%, when using 2.6 × 10⁻⁵ mol catalyst (1.0% with respect to ArN₃) under reflux of the substrate and in 0.5 to 6 hours interval. As mechanism is concerned, a bis-imido ruthenium(VI) intermediate is responsible for the nitrene transfer reaction.

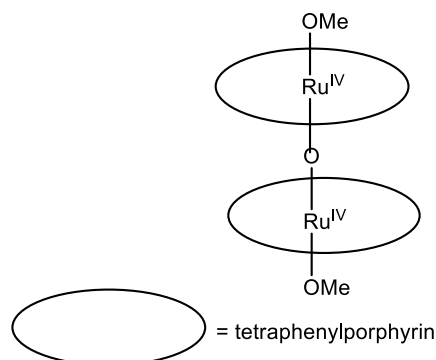


Figure 14. Sandwich-type ruthenium(IV) μ -oxo porphyrin complexes.

The direct amidation of a wide range of aldehydes using [*N*-(*p*-tolylsulfonyl)imino]phenyliodinane (PhI=NTs) as a nitrogen source was catalysed successfully by ruthenium(II)-tetratolyl-(CO)-porphyrins [Ru(TTP)(CO)]²⁹ (Figure 15). The authors concluded that the amidation only occurs at the acyl C-H bond of the starting aldehyde. The reaction conditions are mild; room temperature is acceptable, the yields vary from 68 to 99%, and the molar ratio of catalyst: aldehyde: nitrogen source = 1:10:20.

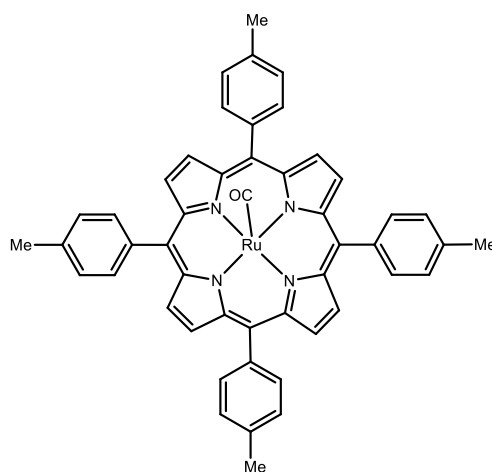
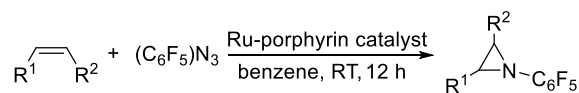


Figure 15. Ruthenium(II)-tetratolyl-(CO)-porphyrin.

Alkene aziridation with pentafluorophenyl azide (Scheme 7) required 0.5 mol% Ru(IV)-[tetrakis(4-fluorophenyl)porphyrin](1,3-dimethyl-2,3-dihydro-1H-benzimidazol-2-ylidene)₂ (Figure 9) as catalyst, benzene as solvent, without heating. Yields between 92 and 99% were obtained for several alkenes investigated, under these very mild conditions.



Scheme 7. General alkene aziridation reaction.

Asymmetric aziridination of aromatic alkenes and asymmetric amidation of benzylic hydrocarbons was achieved using chiral ruthenium porphyrins feature aziridine selectivities for aromatic alkenes and amide

selectivities for benzylic hydrocarbons.³⁰ The porphyrin catalyst (Haltermann porphyrin) (Figure 16) contains a sterically demanding D_4 -symmetric chiral ligand: 5,10,15,20-tetrakis-{(1*S*,4*R*,5*R*,8*S*)-1,2,3,4,5,6,7,8-octahydro-1,4:5,8-dimethanoanthracene-9-yl}porphyrin and two tosylimido axial ligands:

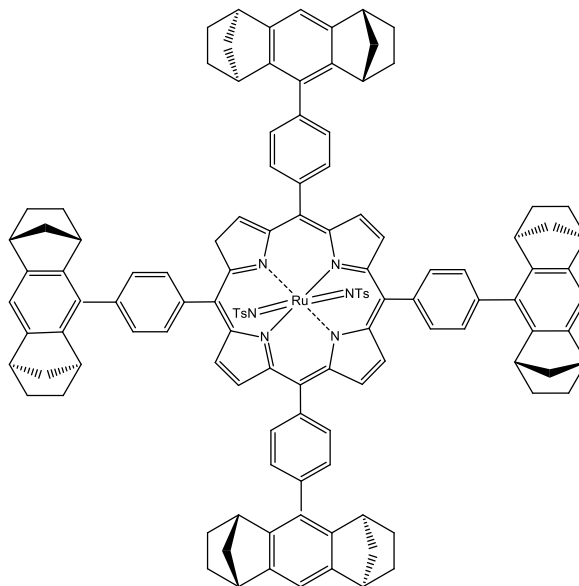
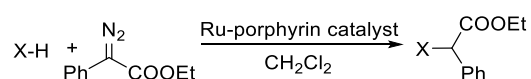


Figure 16. Haltermann porphyrin.

Kinetic studies performed by the authors show a significant effect of the large porphyrin ligand on the nitrogen-atom-transfer reactions of bis(tosylimido)ruthenium(VI) porphyrins.

3.5. Insertion reactions

The ruthenium(II)-tetratolyl-(CO)-porphyrins [Ru(TTP)(CO)]²⁹ were also tested as catalysts for carbene X-H insertion reactions (Scheme 8). Good yields (over 55%) were obtained for a series of substrates.



Scheme 8. General carbene X-H insertion reaction.

For example, the reaction between ethyl 2-diazo-2-phenylacetate and thiophenol gave 98% yield when using 2 mol% Ru(IV)-tetra-(4-fluorophenyl)porphyrin(1,3-dimethyl-2,3-dihydro-1H-benzimidazol-2-ylidene)₂ (Figure 9) as catalyst and dichloromethane as solvent. The reaction was completed in four hours, at room temperature.

In order to obtain more active and less oxygen-sensitive catalyst for carbene transfer reactions, the modification of wild-type myoglobin (Mb) through the insertion of a Ru mesoporphyrin IX into the active site was performed.³¹ The experiments proved that the obtained RuMb can be an effective catalyst for N-H insertion and for carbene transfer reactions, but has less stability and a reduced lifetime compared to the iron-containing analogues.

Ru(IV)-*meso*-tetrakis(pentafluorophenyl)-porphyrin chloride (Figure 17) can catalyze inter- and intramolecular nitrene insertion into sp^3 C-H bonds of hydrocarbons in good to high product yields using

phosphoryl azides as nitrene sources.³² The optimum reaction conditions are: phosphoryl azide 0.2 mmol; hydrocarbon 4 mmol (20 equiv.); ruthenium catalyst 2 mol%; 4 Å molecular sieves 100 mg; dichloroethane 3 mL; argon, reflux; 12 h.

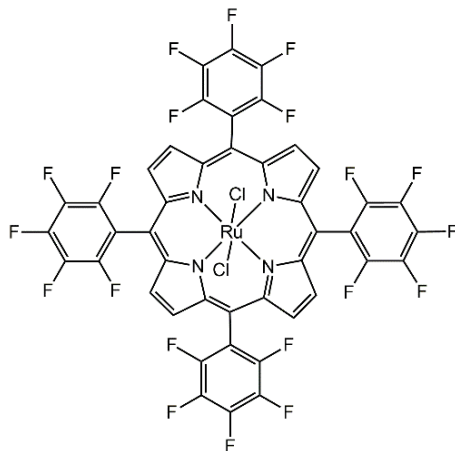
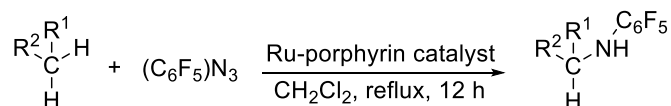


Figure 17. Ru(IV)-tetra(pentafluorophenyl)-porphyrin chloride.

Nitrene insertion into saturated C-H bonds with pentafluorophenyl azide was also obtained using 0.5 mol% Ru(IV)-tetra-(4-fluorophenyl)porphyrin(1,3-dimethyl-2,3-dihydro-1*H*-benzimidazol-2-ylidene)₂ (Figure 9) catalyst, dichloromethane as solvent and 12 hours reflux yielded over 88% product, when tested on different aliphatic and aromatic substrates, from cyclohexane (90%) to 1,2,3,4-tetrahydronaphthalene (96%).



Scheme 9. General nitrene insertion reaction.

3.6. Oxidation reactions

A complex and detailed study performed by Gross and Ini³³ concerning the intermediate species that have definitive role in the epoxidation reaction of olefins by aromatic *N*-oxides catalysed by ruthenium-porphyrins, established that the *N*-oxide-coordinated oxoruthenium(IV) complexes are the most reactive as well as most selective intermediates.

Enantioselective epoxidation reactions of 3-alkenylquinolones were achieved with the three chiral ruthenium porphyrin complexes shown in Figure 18.³⁴

Compound 1 (Figure 25) exhibited excellent catalytic properties in the enantioselective epoxidation of 3-vinylquinolone (95% ee with a 1 mol % catalyst loading), and by comparison to catalyst 2 (Figure 18), it could be shown that the enantioselectivity is due to the presence of two hydrogen bonding sites at a chiral bifunctional ligand.

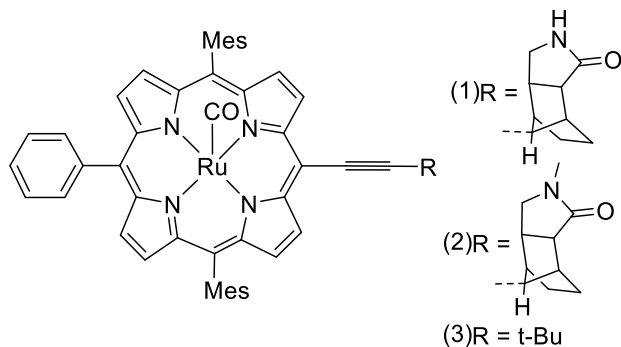


Figure 18. Ruthenium porphyrin complexes.

As Ir(III)-porphyrins have the capacity to bind axial ligands that can modulate the electronic properties of the metal ion, introducing N-heterocyclic carbene (NHC) ligands into the axial position of Ir(III)-porphyrins, modifies the photophysical properties of the obtained compounds such as: split Soret bands, broadened and redshifted absorption and emission spectra and substantially reduced emission quantum yield and lifetime.³⁵ A deformation of the porphyrin ring takes place in order to relieve the steric repulsion between the NHC ligands and the porphyrin ring. Bis-NHC complexes: bis(1,3-dimethyl-2,3-dihydro-1*H*-imidazol-2-ylidene)-(tetratolylporphyrinato)iridium [Ir(ttp)(IME)₂]⁺ (Figure 19), and bis(1,3-dimethyl-2,3-dihydro-1*H*-benzimidazol-2-ylidene)-(2,3,7,8,12,13,17,18-octaethylporphyrinato)-iridium [Ir(oep)(BIME)₂]⁺ are able to catalyse the photoinduced aerobic oxidation of a variety of secondary amines and arylboronic acids. Conditions for secondary amine oxidation: dibenzylamine (0.1 mmol) and catalyst (0.1 mmol) in MeCN (1.5 mL), O₂ bubbling, xenon lamp (>400 nm). Using the bulkier Ir-porphyrin compound [Ir(oep)(BIME)₂]⁺ led to a better yield (99%) as compared to the 92% obtained for the [Ir(ttp)(IME)₂]⁺ counterpart. Conditions for arylboronic acid oxidation: arylboronic acid (0.1 mmol), diisopropylamine (0.4 mmol) and [Ir(oep)(BIME)₂]⁺ (0.5 mmol) in DMF (1.5 mL), O₂ bubbling, xenon lamp (>400 nm), when 100% conversion was registered.

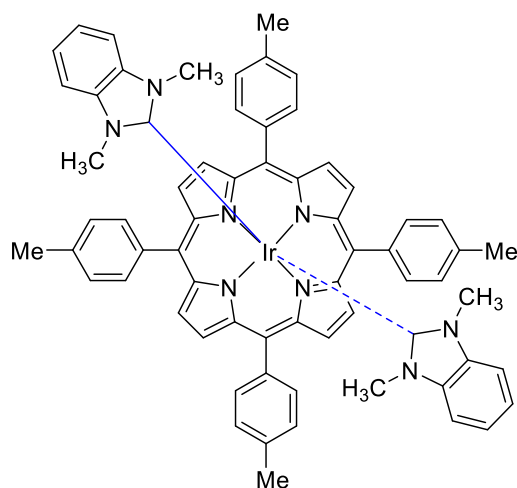


Figure 19. Bis(1,3-dimethyl)-2,3-dihydro-1*H*-imidazol-2-ylidene)-(tetratolylporphyrinato)-iridium.

4. Hydrogen Evolution and Water Oxidation Catalysed by Pt- and Pd-porphyrin Hybrids

Solar-driven water splitting to produce O₂ and H₂ by means of photoelectrochemical cells represents an alternative source of fuels for the future. To perform this task, the cells must contain a material capable of light harvesting, one for catalysing light-driven water oxidation and one for proton reduction.³⁶

A Pt(II)-triphenylporphyrin with a 2-bromopropionate group attached to the fourth phenyl substituent in meso position in order to restrain H-aggregation (Figure 20) was assembled onto multiwalled carbon nanotubes.³⁷ The hybrid material was tested as electrocatalyst for the hydrogen evolution reaction (HER). The as-prepared composites exhibit superior HER catalytic activity with an overpotential of 35 mV for an electrocatalytic current density of $j = -10 \text{ mA cm}^{-2}$ and a Tafel slope of 32.3 mV dec^{-1} . Moreover, such catalysts do not exhibit observable activity decay after a 1000-cycle stability test, thus demonstrating their excellent durability.

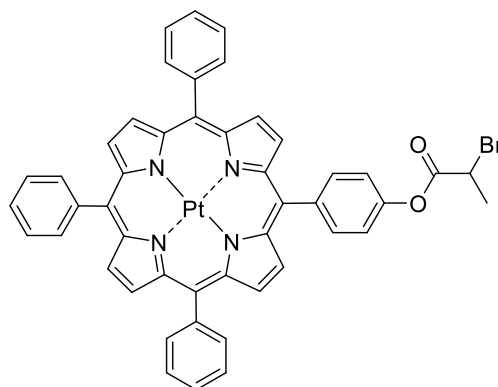


Figure 20. 5-[4-(2-Bromopropanoyloxy)phenyl]-10,15,20-triphenylporphyrin-Pt(II).

Among the photocatalysts that are able to convert solar energy into renewable fuels, gel catalysts present the advantage of large surface areas and allow for the adsorption and dissociation of water.³⁸ The authors obtained porphyrin-imine gels by reacting 5,10,15,20-tetrakis(*p*-aminophenyl)porphyrin and its Pd and SnCl₂-metallated derivatives with 1,3,5-tris-(4-formylphenyl)triazine (TFPT). The amine groups of the porphyrin act as functional ends for the bond with polymeric imine gels. The nanomaterials were completely morphologically characterized and then used as photocatalysts for hydrogen evolution in an aqueous system using ascorbate as sacrificial electron donor and platinum as cocatalyst. It was concluded that the gel containing the porphyrin base had the lowest hydrogen production rate, of only $29 \mu\text{mol h}^{-1} \text{ g}^{-1}$, the wet gel containing Sn-porphyrin showed continuous and stable hydrogen production of only $65 \mu\text{mol h}^{-1} \text{ g}^{-1}$ during continuous 24 h visible light illumination ($\lambda > 420 \text{ nm}$), whereas the imine gel containing Pd-porphyrin and Pt cocatalyst (Pt-doped PdTAPP-TFPT) presented a rate of $671 \mu\text{mol h}^{-1} \text{ g}^{-1}$ in the same conditions. The production of hydrogen photocatalyzed by Pt-doped PdTAPP-TFPT was continuous for 4 runs and presented a good stability.

The need for more photostable photosensitizers able to initiate the oxidation of water in phosphate buffer determined Brouwer *et al.*³⁹ to design a three-component system, in which Pt(II)-tetra(4-carboxyphenyl)porphyrin or the corresponding tetramethyl ester act as photoanode, in combination with both homogeneous (Ir-NHC and Co₄O₄-cubane complexes) and heterogeneous water oxidation catalysts (IrO_x·nH₂O ~2 nm and Co₃O₄ nanoparticles, ~50 nm) and sodium persulfate as sacrificial electron acceptor.

It was concluded that Pt(II)-meso[tetra(4-methoxycarbonyl)phenyl]porphyrin has three times the photon capture ability and 240 mV more oxidizing power than the extensively used tris(2,2'-bipyridyl)ruthenium(II) [Ru(bpy)₃²⁺].⁴⁰

In the desire to create better supported catalysts for an improved photocatalytic H₂ evolution in which the loading of the active ingredient can be increased, without the prospect of its aggregation due to thermal instability, a two-dimensional metal-organic framework (MOF) coordinating the catalyst in ultrahigh concentration was designed.⁴¹ The MOF was obtained by a bottom-up coordination procedure using Pt(II)-tetrakis(4-carboxyphenyl)porphyrin as a linker and Cu₂(COO)₄ paddle-wheel clusters as the metal nodes and polyvinyl pyrrolidone (PVP) as surfactant. PVP attached on the surface of the formed MOF and could prevent the stacking, favouring the formation of thin MOF sheets. These provide accessible active sites and higher photocatalytic performance due to the prevention of undesired electron-hole recombination. The Pt content was determined to be 12.0 wt%. Water splitting photocatalyzed by these Pd-catalyst loaded MOF sheets under visible light irradiation ($\lambda > 420$ nm) and using ascorbic acid as sacrificial agent produced hydrogen at a rate of 11320 $\mu\text{mol}\cdot\text{g}^{-1}\cdot\text{h}^{-1}$, that is significantly higher than other MOF-based photocatalysts, and the material could be recycled four times without significant loss of activity. The material also presents high dispersity in ethanol and can be drop-cast in thin films onto solid substrates without loss of activity.

The synergetic effect between Pd-porphyrin photosensitizers and Pt-NP cocatalysts confined within nanoscale coordination interspaces incorporating hydrophilic Hf(IV)-oxo clusters⁴² led to a H₂ evolution rate of 22674 $\mu\text{mol}\cdot\text{g}^{-1}\cdot\text{h}^{-1}$ with turn-over number (TON) of 4131.2 in 32 h and highest turn-over frequency (TOF) of 482.5 h⁻¹. The Pd-porphyrin metalorganic framework was obtained hydrothermally from Pd(II)-tetrakis-(4-carboxyphenyl)porphyrin and HfCl₄ and into this network PtNPs were introduced. The obtained hybrid nanomaterial was morphologically and electrochemically characterized and its excellent performance determined the presentation of a reaction mechanism: under visible light excitation, the electrons transfer from the LUMO of Pd-porphyrin ligand to Pt-NPs, where the H₂O molecules were reduced to generate H₂. On the other hand, the Hf(IV)-based MOF provided hydrophilic Hf(IV)-oxo clusters with H₂O accumulation for photocatalytic water splitting.

5. Conclusions

While porphyrin platinum metal complexes catalyze a range of useful organic transformations, including C-C bond forming reactions, they excel at the oxidation and functionalization of hydrocarbonate substrates for which there exist few alternative catalysts. Combined with light harvesting moieties, they allow for water splitting, thus providing a potentially viable and commercially attractive alternative to electrolysis. Furthermore, essentially quantitative and highly selective oxidations of hydrocarbons with solid-supported porphyrin complexes provide an entry into industrially useful intermediates under milder conditions and with excellent atom economy. Achieving similar milestones in the corresponding amination reactions would only increase the attractiveness of these catalysts.

However, in order to realize the full potential of such applications, combined synthetic and engineering teamwork is needed to increase the range of substrates amenable to such transformations, improve the efficiency of the electron transfer reactions, the robustness of the catalysts under practical scenarios, and demonstrate economically feasible implementation at scale.

6. Acknowledgements

This research is funded by UEFISCDI, project ECOTECH-GMP 76 PCCDI/2018, belonging to PNIII-Future and Emerging Technologies and partially by the Romanian Academy through Program 3/2020 from the Institute of Chemistry "Coriolan Dragulescu".

References

1. Mironov, A. *Handbook of Porphyrin Science* **2012**, *18*, 303–413.
https://doi.org/10.1142/9789814335508_0012
2. Wan, Q.-X.; Liu, Y. *Catal. Lett.* **2008**, *128*, 487–492.
<https://doi:10.1007/s10562-008-9780-2>
3. Rao, K. U.; Lakshmidivi, J.; Appa, R. M.; Prasad, S. S.; Narasimhulu, M.; Vijitha, R.; Rao K.S.V.K.; Venkateswarlu, K. *Chemistry Select* **2017**, *2*, 7394–7398.
<https://doi:10.1002/slct.201701413>
4. Zhang, J.; Zhao, G.-F.; Popović, Z.; Lu, Y.; Liu, Y. *Mater. Res. Bull.* **2010**, *45*, 1648–1653.
<https://doi:10.1016/j.materresbull.2010.07.006>
5. Venkateswarlu, K.; Rao, K. *Synlett* **2018**, *29*, 1055–1060.
<https://doi:10.1055/s-0036-1591549>
6. Kostas, I. D.; Coutsolelos, A. G.; Charalambidis, G.; Skondra, A. *Tetrahedron Lett.* **2007**, *48*, 6688–6691.
<https://doi:10.1016/j.tetlet.2007.07.141>
7. Bahrami, K.; Kamrani, S. N. *Appl. Organomet. Chem.* **2017**, *32*, e4102.
<https://doi:10.1002/aoc.4102>
8. Fareghi-Alamdari, R.; Golestanzadeh, M.; Bagheri, O. *RSC Advances* **2016**, *6*(110), 108755–108767.
<https://doi:10.1039/c6ra21223a>
9. Bagheri, O.; Sadegh, F.; Moghadam, M.; Tangestaninejad, S.; Mirkhani, V.; Mohammadpoor-Baltork, I.; Safiri, M. *Appl. Organomet. Chem.* **2014**, *28*, 337–346.
<https://doi:10.1002/aoc.3131>
10. Sadegh, F.; Bagheri, O.; Moghadam, M.; Mirkhani, V.; Tangestaninejad, S.; Mohammadpoor-Baltork, I. *J. Organomet. Chem.* **2014**, *759*, 46–57.
<https://doi:10.1016/j.jorganchem.2014.02.006>
11. Fujimoto, K.; Yoneda, T.; Yorimitsu, H.; Osuka, A. *Angew. Chem. Int. Ed.* **2013**, *53*, 1127–1130.
<https://doi:10.1002/anie.201308551>
12. Suijkerbuijk, B. M. J. M.; Herreras Martínez, S. D.; Koten, G. van; Klein Gebbink, R. J. M. *Organometallics* **2008**, *27*, 534–542.
<https://doi:10.1021/om7005613>
13. Venkateswarlu, K.; Rao, K. *Synlett* **2018**, *29*, 1055–1060.
<https://doi:10.1055/s-0036-1591549>
14. Dela Cruz, J.; Ruamps, M.; Arco, S.; Hung, C.-H. *Dalton Trans.* **2019**, *48*, 7527–7531.
<https://doi:10.1039/c9dt00104b>
15. Xie, M.-H.; Yang, X.-L.; Wu, C.-D. *Chem. Commun.* **2011**, *47*, 5521.
<https://doi:10.1039/c1cc10461f>

16. To, W.-P.; Liu, Y.; Lau, T.-C.; Che, C.-M. *Chem. Eur. J.* **2013**, *19*, 5654–5664.
<https://doi:10.1002/chem.201203774>
17. Thompson, S. J.; Brennan, M. R.; Lee, S. Y.; Dong, G. *Chem. Soc. Rev.* **2018**, *47*, 929–981.
<https://doi:10.1039/c7cs00582b>
18. Liu, J.; Fan, Y.-Z.; Li, X.; Wei, Z.; Xu, Y.-W.; Zhang, L.; Su, C.-Y. *Appl. Catal. B.* **2018**, *231*, 173–181.
<https://doi:10.1016/j.apcatb.2018.02.055>
19. Sun, D.; Gao, Y.; Fu, J.; Zeng, X.; Chen, Z.; Li, Z. *Chem. Commun.* **2015**, *51*, 2645–2648.
<https://doi:10.1039/c4cc09797a>
20. Epp, K.; Bueken, B.; Hofmann, B.; Cokoja, M.; Hemmer, K.; De Vos, D. E.; Fischer, R. A. *Catal. Sci. Technol.* **2019**, *11*, 6452–6459.
<https://doi:10.1039/c9cy00893d>
21. Chan, K.-H.; Guan, X.; Lo, V. K.-Y.; Che, C.-M. *Angew. Chem. Int. Ed.* **2014**, *53*, 2982–2987.
<https://doi:10.1002/anie.201309888>
22. Nicolas, I.; Maux, P. L.; Simonneaux, G. *Tetrahedron Lett.* **2008**, *49*, 5793–5795.
<https://doi:10.1016/j.tetlet.2008.07.133>
23. Kroitor, A. P.; Cailler, L. P.; Martynov, A. G.; Gorbunova, Y. G.; Tsivadze, A. Y.; Sorokin, A. B. *Dalton Trans.* **2017**, *46*, 15651–15655.
<https://doi:10.1039/c7dt03703a>
24. Wang, H.; Wan, Q.; Low, K.-H.; Zhou, C.; Huang, J.-S.; Zhang, J.-L.; Che, C.-M. *Chem. Sci.*, **2020**, *11*, 2243.
<https://doi:10.1039/c9sc05432d>
25. Che, C.-M.; Huang, J.-S. *Coord. Chem. Rev.* **2002**, *231*, 151–164.
[https://doi:10.1016/s0010-8545\(02\)00117-0](https://doi:10.1016/s0010-8545(02)00117-0)
26. Wang, C.; Shalyaev, K. V.; Bonchio, M.; Carofiglio, T.; Groves, J. T. *Inorg. Chem.* **2006**, *45*, 4769–4782.
<https://doi:10.1021/ic0520566>
27. Fantauzzi, S.; Caselli, A.; Gallo, E. *Dalton Trans.* **2009**, *28*, 5434.
<https://doi:10.1039/b902929j>
28. Zardi, P.; Intrieri, D.; Carminati, D. M.; Ferretti, F.; Macchi, P.; Gallo, E. *J. Porphyr. Phthaloc.* **2016**, *20*(08n11), 1156–1165.
<https://doi:10.1142/s1088424616500814>
29. Chang, J. W. W.; Chan, P. W. H. *Angew. Chem. Int. Ed.* **2008**, *47*, 1138–1140.
<https://doi:10.1002/anie.200704695>
30. Liang, J.-L.; Huang, J.-S.; Yu, X.-Q.; Zhu, N.; Che, C.-M. *Chem. Eur. J.* **2002**, *8*, 1563–1572.
[https://doi:10.1002/1521-3765\(20020402\)8:7<1563::AID-CHEM1563>3.0.CO;2-V](https://doi:10.1002/1521-3765(20020402)8:7<1563::AID-CHEM1563>3.0.CO;2-V)
31. Wolf, M. W.; Vargas, D. A.; Lehnert, N. *Inorg. Chem.* **2017**, *56*(10), 5623–5635.
<https://doi:10.1021/acs.inorgchem.6b03148>
32. Xiao, W.; Wei, J.; Zhou, C.-Y.; Che, C.-M. *Chem. Commun.* **2013**, *49*, 4619.
<https://doi:10.1039/c3cc41110a>
33. Gross, Z.; Ini, S. *Inorg. Chem.* **1999**, *38*, 1446–1449.
<https://doi:10.1021/ic981021l>
34. Fackler, P.; Huber, S. M.; Bach, T. *J. Am. Chem. Soc.* **2012**, *134*, 12869–12878.
<https://doi:10.1021/ja305890c>
35. Lam, T. L.; Ka Chung, T.; Yang, C.; Kwong, W.-L.; Guan, X.; Li, M.-D.; Lo, V. K.-Y.; Chan, S. L.-F.; Phillips, D. L.; Lok, C.-N.; Che, C.-M. *Chem. Sci.* **2019**, *10*, 293–309.
<https://doi:10.1039/c8sc02920b>

36. Shen, S.; Lindley, S. A.; Dong, C.; Chen, E.; Lu, Y.; Zhou, J.; Hu, Y.; Wheeler, D.A.; Guo P.; Zhang J.Z.; Kliger D.S.; Mao, S. S. *Solar RRL*, **2018**, 1800285.
<https://doi:10.1002/solr.201800285>
37. Wang, L.; Zhang, Z.; Li, M.; Li, Q.; Wang, B.; Wang, S.; Zhou, H.; Mao, B. *ChemCatChem* **2020**,
<https://doi:10.1002/cctc.202000104>
38. Liao, P.; Hu, Y.; Liang, Z.; Zhang, J.; Yang, H.; He, L.-Q.; Tong Y.-X.; Liu, J.-M.; Chen, L.; Su, C.-Y. *J Mat. Chem. A* **2018**, *6*, 3195–3201.
<https://doi:10.1039/c7ta09785a>
39. Chen, H.-C.; Hettler, D. G. H.; Williams, R. M.; van der Vlugt, J. I.; Reek, J. N. H.; Brouwer, A. M. *Energy Environ. Sci.* **2015**, *8*, 975–982.
<https://doi:10.1039/c4ee03302g>
40. Wacholtz, W. F.; Auerbach, R. A.; Schmehl, R. H. *Inorg. Chem.* **1986**, *25*, 227–234.
<https://doi:10.1021/ic00222a027>
41. Zuo, Q.; Liu, T.; Chen, C.; Ji, Y.; Gong, X.; Mai, Y.; Zhou, Y. *Angew. Chem. Int. Ed. Engl.* **2019**, *58*, 10198–10203.
<https://doi:10.1002/ange.201904058>
42. Li, S.; Mei, H.-M.; Yao, S.-L.; Chen, Z.; Lu, Y.-L.; Zhang, L.; Su, C.-Y. *Chem. Sci.* **2019**, *10*, 10577–10585.
<https://doi:10.1039/c9sc01866b>

Author's Biography



Lascu Anca is currently third-degree scientific researcher at the Institute of Chemistry “Coriolan Dragulescu” Timisoara of the Romanian Academy. She graduated Industrial Chemistry and Environmental Engineering Faculty, Timisoara, Romania in 1992 as chemical engineer and was awarded PhD title in 2010 in chemistry. Since 2013 she has been involved in research of porphyrin synthesis and applications.

This paper is an open access article distributed under the terms of the Creative Commons Attribution (CC BY) license (<http://creativecommons.org/licenses/by/4.0/>)